Preamble-based Channel Estimation in MIMO-OFDM/OQAM Systems

Eleftherios Kofidis [1], Dimitrios Katselis [2]

[1] *Department of Statistics and Insurance Science,*
University of Piraeus,
185 34 Piraeus, Greece.
kofidis@unipi.gr

[2] *ACCESS Linnaeus Center,*
School of Electrical Engineering, Royal Institute of Technology (KTH),
SE 100-44, Sweden.
dimitrik@kth.se

***Abstract*—Filter bank-based multicarrier modulation (FBMC) using offset quadrature amplitude modulation (OQAM), known as OFDM/OQAM (or FBMC/OQAM), provides an attractive alternative to the conventional cyclic prefix-based orthogonal frequency division multiplexing (CP-OFDM), especially in terms of increased robustness to frequency offset and Doppler spread, and high bandwidth efficiency. It suffers, however, from an inherent (intrinsic) imaginary inter-carrier/inter-symbol interference that complicates signal processing tasks such as channel estimation (CE). Recently, the so-called interference approximation method (IAM) was proposed for preamble-based CE in single-input single-output (SISO) systems. It relies on the knowledge of the pilot's neighborhood to approximate this interference and constructively exploit it in simplifying CE and improving its performance. A number of IAM preambles have been proposed, with varying CE performance. This paper is concerned with the application of the IAM idea in multi-input multi-output (MIMO) systems. The most prominent IAM variants are considered and their MIMO extensions with their relative advantages and practical issues are investigated. The IAM preambles are compared, with each other and with CP-OFDM, via simulations in both mildly and highly frequency-selective channels.**

I. Introduction

Orthogonal frequency division multiplexing (OFDM) has become quite popular in both wired and wireless communications [1], [3], mainly because of its immunity to multipath fading, which allows a significant increase in the transmission rate [20]. Using the cyclic prefix (CP) as a guard interval, OFDM manages to turn a frequency selective channel into a set of parallel flat channels with independent noises. This greatly simplifies both the estimation of the channel and the recovery of the transmitted data at the receiver. However, these advantages come at the cost of an increased sensitivity to frequency offset and Doppler spread. This is due to the fact that, although the subcarrier functions are perfectly localized in time, they suffer from spectral leakage in the frequency domain and hence inter-carrier interference (ICI) results. Moreover, the inclusion of the CP entails a waste in transmitted power as well as in spectral efficiency, which, in practical systems, can go up to 25% [3].

Filter bank-based multicarrier modulation (FBMC) using offset quadrature amplitude modulation (OQAM), known as OFDM/OQAM [18], provides an alternative to CP-OFDM, that can mitigate these drawbacks. OFDM/OQAM employs pulse shaping via an IFFT/FFT-based efficient filter bank, and staggered OQAM symbols, i.e., real symbols at twice the symbol rate of OFDM/QAM, are loaded on the subcarriers [18]. This allows for the pulses to be well localized in *both* the time and the frequency domains while still keeping maximum spectral efficiency [10]. As a consequence, the system's robustness to frequency offsets and Doppler effects is increased and at the same time an enhanced spectral containment, for bandwidth sensitive applications (e.g., cognitive radio [2], [10]), is offered. Moreover, OFDM/OQAM does not require the inclusion of a CP, which may lead to even higher transmission rates [18], [17].

However, the subcarrier functions are now only orthogonal in the *real* field, which means that there is always an *intrinsic* imaginary interference among (neighboring) subcarriers and symbols [13]. As a consequence, the simplicity of the channel estimation (CE) in CP-OFDM is lost in OFDM/OQAM systems, as the real-valued pilots are also "polluted" by this imaginary-valued contribution of their neighbors. A number of training schemes and associated CE methods that take this into account have recently appeared in the literature, including both preamble-based (e.g., [15], [16]) and scattered pilots-based (e.g., [13], [4]) ones. These can be roughly characterized as aiming at cancelling the undesired interference or constructively exploiting it to improve the estimation performance. The latter approach relies on the fact that the interference to a pilot symbol is mainly contributed to by its first-order neighbors, and hence it can be approximated if these neighbors also carry known symbols, a not uncommon situation within a preamble. This has been known as the Interference Approximation Method (IAM) [15]. The idea is to combine the real-valued pilot with the interference approximation into a complex-valued *pseudo-pilot* and performing CE as in CP-

This is part of the work done by the authors within the FP7 project PHYDYAS (http://www.ict-phydyas.org) as members of the partner RA-CTI, Greece, and in collaboration with the Dept. of Informatics and Telecommunications of the University of Athens, Greece.

978-1-4577-0242-6/11/$26.00 ©2011 IEEE

OFDM, under the assumption of a locally constant channel frequency response. As the pseudo-pilot divides the noise component, its magnitude should be as large as possible. This way, the interference turns into a benefit for the CE task and hence the neighboring pilots should be so chosen as to maximize its effect.

A number of variants of IAM have been proposed, corresponding to different choices for the preamble structure [14], [9]. Those that have received most of the attention comprise three OFDM/OQAM symbols (i.e., 1.5 complex OFDM/QAM symbols), with the side ones being all zeros. This is to protect the middle vector of pilots from being interfered by the unknown data parts of the previous and current frames. The middle pilot symbols are then chosen so as to maximize the interference contributions from neighboring subcarriers.

To the best of the authors' knowledge, CE for MIMO-OFDM/OQAM systems has so far only been considered with scattered pilots [11], [12], based on the concept of help pilot developed in [13]. This paper considers preamble-based CE for MIMO-OFDM/OQAM, extending IAM to the MIMO case. The most prominent IAM variants of the above 3-symbol type are considered and their MIMO extensions with their relative advantages and practical issues are investigated. The MIMO IAM preambles are compared, with each other and with CP-OFDM, via simulations in both mildly and highly frequency-selective channels.

The rest of the paper is organized as follows: In Section II, the discrete-time baseband equivalent model for the OFDM/OQAM system is described. Section III reviews the main IAM approaches for structuring the preamble and exploiting it for SISO channel estimation. The MIMO case is addressed in Section IV. Simulation results are reported in Section V.

Notation. Vectors and matrices are denoted by bold lowercase and uppercase letters, respectively. Superscript ^{T} stands for transposition. The complex conjugate of a complex number z is denoted by $z^\star$. Also, $\jmath = \sqrt{-1}$. $\|\cdot\|$ is the Frobenius norm. $\otimes$ denotes the (left) Kronecker product. The expectation operator is denoted by $E(\cdot)$. $\boldsymbol{I}_m$ denotes the mth-order identity matrix.

II. System Model

The (QAM or OQAM)OFDM modulator output is transmitted through a channel of length L_h, which is assumed to be invariant in the duration of the preamble. At the receiver front-end, noise is added, which is assumed Gaussian with zero mean and variance σ^2. For CP-OFDM, the classical configuration is assumed [20]. The discrete-time signal at the output of the OFDM/OQAM synthesis filter bank (SFB) is given by [18]

$$s(l) = \sum_{m=0}^{M-1} \sum_n d_{m,n} g_{m,n}(l), \tag{1}$$

where $d_{m,n}$ are *real* OQAM symbols, and

$$g_{m,n}(l) = g\left(l - n\frac{M}{2}\right) e^{\jmath \frac{2\pi}{M} m\left(l - \frac{L_g - 1}{2}\right)} e^{\jmath \varphi_{m,n}},$$

with g being the *real symmetric* prototype filter impulse response (assumed here of unit energy) of length L_g, M being the *even* number of subcarriers, and $\varphi_{m,n} = \varphi_0 + \frac{\pi}{2}(m+n) \bmod \pi$, where φ_0 can be arbitrarily chosen [18]. In this paper, and without loss of generality, $\varphi_{m,n}$ is defined as $(m+n)\frac{\pi}{2} - mn\pi$ as in [18]. The filter g is usually designed to have length $L_g = KM$, with K being the overlapping factor. The double subscript $(\cdot)_{m,n}$ denotes the (m,n)-th frequency-time (FT) point. Thus, m is the subcarrier index and n the OQAM symbol time index.

The pulse g is designed so that the associated subcarrier functions $g_{m,n}$ are orthogonal in the *real* field [18]. This implies that even in the absence of channel distortion and noise, and with perfect time and frequency synchronization, there will be some intercarrier (and/or intersymbol) interference at the output of the analysis filter bank (AFB), which is purely imaginary (the notation in [15] is adopted):

$$\sum_l g_{m,n}(l) g_{p,q}^\star(l) = \jmath \langle g \rangle_{m,n}^{p,q}, \tag{2}$$

and known as *intrinsic* interference [13]. Making the common assumption that the channel is (approximately) frequency flat at each subcarrier and constant over the duration of the prototype filter [15], which is true[1] for practical values of L_h and L_g and for well time-localized g's, one can express the AFB output at the pth subcarrier and qth OFDM/OQAM symbol as:

$$y_{p,q} = H_{p,q} d_{p,q} + \underbrace{\jmath \underbrace{\sum_{m=0}^{M-1} \sum_n}_{(m,n)\neq(p,q)} H_{m,n} d_{m,n} \langle g \rangle_{m,n}^{p,q}}_{I_{p,q}} + \eta_{p,q} \tag{3}$$

where $H_{p,q}$ is the M-point channel frequency response (CFR) at that FT point, and $I_{p,q}$ and $\eta_{p,q}$ are the associated interference and noise components, respectively. $\eta_{p,q}$ has been shown to be stationary (in fact, also Gaussian with zero mean and variance σ^2) and correlated among adjacent subcarriers (see [6]). This correlation will be henceforth assumed negligible, a valid assumption for well frequency-localized prototype filters.

A common assumption is that, with a well time-frequency localized pulse, contributions to $I_{p,q}$ only come from the first-order neighborhood of (p,q), namely $\Omega_{p,q} = \{(p\pm 1, q\pm 1), (p, q\pm 1), (p\pm 1, q)\}$. If, moreover, the CFR is almost constant over this neighborhood, one can write (3) as

$$y_{p,q} \approx H_{p,q} c_{p,q} + \eta_{p,q} \tag{4}$$

where

$$c_{p,q} = d_{p,q} + \jmath \underbrace{\sum_{(m,n)\in\Omega_{p,q}} d_{m,n} \langle g \rangle_{m,n}^{p,q}}_{u_{p,q}} = d_{p,q} + \jmath u_{p,q}, \tag{5}$$

[1] This is not an accurate subchannel model in case M, the number of subcarriers, is not large enough with respect to the frequency selectivity of the channel (see Section V for such examples). This is also the case in high mobility scenarios, where M should be small, to cope with ICI from frequency dispersion.

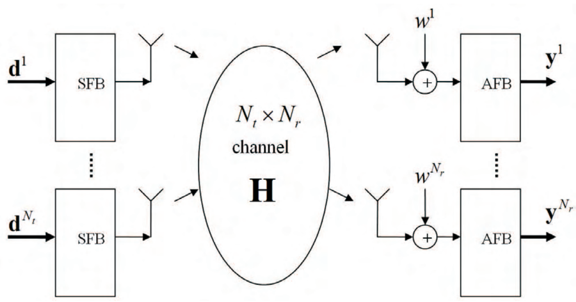

Fig. 1. The MIMO-OFDM/OQAM system.

is the *virtual* transmitted symbol at (p, q), with

$$u_{p,q} = \sum_{(m,n)\in\Omega_{p,q}} d_{m,n}\langle g\rangle_{m,n}^{p,q} \tag{6}$$

being the imaginary part of the interference from the neigboring FT points. When known pilots are transmitted at that FT point and its neighborhood $\Omega_{p,q}$, the quantity in (5) can be approximated. This can then serve as a *pseudo pilot* [15] to compute an estimate of the CFR at the corresponding FT point, as, for example,

$$\hat{H}_{p,q} = \frac{y_{p,q}}{c_{p,q}} \approx H_{p,q} + \frac{\eta_{p,q}}{c_{p,q}} \tag{7}$$

This observation underlies the IAM schemes to be described in the sequel.

The above formulation can be easily extended to the MIMO case. Consider an $N_\mathrm{t} \times N_\mathrm{r}$ MIMO system, with identical modulators (demodulators) at each transmit (receive) antenna (see Fig. 1) and temporaly/spatially white noise at the receiver front end. Then, with the same assumptions as previously, one can write an equation analogous to (4) for each receive antenna $j = 1, 2, \ldots, N_\mathrm{r}$:

$$y_{p,q}^j = \sum_{i=1}^{N_\mathrm{t}} H_{p,q}^{j,i} c_{p,q}^i + \eta_{p,q}^j, \tag{8}$$

where $H_{p,q}^{j,i}$ is the M-point CFR of the channel from the ith transmit antenna to the jth receive antenna, $c_{p,q}^i$ is the corresponding virtual symbol, and $\eta_{p,q}^j$ denotes the corresponding noise component. Clearly, the latter are uncorrelated among different receive antennas. Collecting the above equations for all receive antennas results, for each FT point, in an input-output equation similar to that for MIMO-OFDM [19]:

$$\boldsymbol{y}_{p,q} = \boldsymbol{H}_{p,q}\boldsymbol{c}_{p,q} + \boldsymbol{\eta}_{p,q}, \tag{9}$$

where

$$\begin{aligned} \boldsymbol{y}_{p,q} &= \begin{bmatrix} y_{p,q}^1 & y_{p,q}^2 & \cdots & y_{p,q}^{N_\mathrm{r}} \end{bmatrix}^T, \\ \boldsymbol{\eta}_{p,q} &= \begin{bmatrix} \eta_{p,q}^1 & \eta_{p,q}^2 & \cdots & \eta_{p,q}^{N_\mathrm{r}} \end{bmatrix}^T, \end{aligned}$$

$$\boldsymbol{H}_{p,q} = \begin{bmatrix} H_{p,q}^{1,1} & H_{p,q}^{1,2} & \cdots & H_{p,q}^{1,N_\mathrm{r}} \\ H_{p,q}^{2,1} & H_{p,q}^{2,2} & \cdots & H_{p,q}^{2,N_\mathrm{t}} \\ \vdots & \vdots & \ddots & \vdots \\ H_{p,q}^{N_\mathrm{r},1} & H_{p,q}^{N_\mathrm{r},2} & \cdots & H_{p,q}^{N_\mathrm{r},N_\mathrm{t}} \end{bmatrix}$$

is the MIMO CFR at that point and

$$\boldsymbol{c}_{p,q} = \boldsymbol{d}_{p,q} + \jmath\boldsymbol{u}_{p,q},$$

with

$$\boldsymbol{d}_{p,q} = \begin{bmatrix} d_{p,q}^1 & d_{p,q}^2 & \cdots & d_{p,q}^{N_\mathrm{t}} \end{bmatrix}^T$$

and $\boldsymbol{u}_{p,q}$ defined similarly.

III. IAM Preambles with Zero Guard Symbols: The SISO Case

One can see from (7) that the preamble should be so structured as to result in pseudo-pilots of *maximum magnitude* [15]. Therefore, the training symbols surrounding the pilot $d_{p,q}$ should be such that all terms in (6) have the same sign so that they add together. Moreover, this should happen for *all* frequencies p.

To this end, one needs to know the interference weights $\langle g\rangle_{m,n}^{p,q}$ for the neighbors $(m, n) \in \Omega_{p,q}$ of each FT point (p, q) of interest. These can be *a priori* computed based on the prototype filter g employed. Moreover, it can be shown that, for *any* choice of g, these weights follow a specific pattern, which, for the definition of φ_0 adopted here, and for *all* q, can be written as[2]

$$\begin{array}{ccc} (-1)^p\delta & -\beta & (-1)^p\delta \\ -(-1)^p\gamma & d_{p,q} & (-1)^p\gamma \\ (-1)^p\delta & \beta & (-1)^p\delta \end{array} \tag{10}$$

with the horizontal direction corresponding to time and the vertical one to frequency. The quantities β, γ, δ are positive and, clearly, smaller than one. Generally, $\beta, \gamma > \delta$. For example, $\gamma = 0.5644$, $\beta = 0.2393$, and $\delta = 0.2058$ for the g's employed in Section V.

A. The IAM-R Method

In order to simplify the task of generating pseudo-pilots of large magnitude, it was suggested in [15], [14] to place nulls at the first and third OFDM/OQAM symbols of the preamble, that is, $d_{p,0} = d_{p,2} = 0$, $p = 0, 1, \ldots, M - 1$. Then, the imaginary part of the pseudo-pilot at $(p, 1)$ will only come from the symbols at the positions $(p \pm 1, 1)$. Obviously, these pilots must be OQAM symbols of maximum modulus, d. Moreover, in view of the pattern (10), they should satisfy the condition $d_{p+1,1} = -d_{p-1,1}$ for all p, in order to yield pseudo-pilots of maximum magnitude, namely $|d_{p,1} + \jmath 2\beta d_{p+1,1}| = d\sqrt{1 + 4\beta^2}$. An example for $M = 8$ and OQPSK modulation is shown in Fig. 2(a). This method is called IAM-R to signify the fact that its pilot symbols are real.

[2]This is without loss of generality as analogous patterns result for other definitions of φ_0.

$$\begin{array}{ccc} 0 & 1 & 0 \\ 0 & -1 & 0 \\ 0 & -1 & 0 \\ 0 & 1 & 0 \\ 0 & 1 & 0 \\ 0 & -1 & 0 \\ 0 & -1 & 0 \\ 0 & 1 & 0 \end{array} \qquad \begin{array}{ccc} 0 & d_0 & 0 \\ 0 & -\jmath d_0 & 0 \\ 0 & -d_0 & 0 \\ 0 & -d_1 & 0 \\ 0 & \jmath d_1 & 0 \\ 0 & d_1 & 0 \\ 0 & -d_0 & 0 \\ 0 & \jmath d_0 & 0 \end{array} \qquad \begin{array}{ccc} 0 & 1 & 0 \\ 0 & -\jmath & 0 \\ 0 & -1 & 0 \\ 0 & \jmath & 0 \\ 0 & 1 & 0 \\ 0 & -\jmath & 0 \\ 0 & -1 & 0 \\ 0 & \jmath & 0 \end{array}$$

(a) (b) (c)

Fig. 2. Preamble structures for (a) IAM-R , (b) IAM-I, and (c) IAM-C methods, for the SISO case. $M = 8$. OQPSK modulation is assumed. d_0, d_1 are randomly chosen BPSK symbols.

$$\begin{array}{ccccc} 0 & 1 & 0 & 1 & 0 \\ 0 & -\jmath & 0 & -\jmath & 0 \\ 0 & -1 & 0 & -1 & 0 \\ 0 & \jmath & 0 & \jmath & 0 \\ 0 & 1 & 0 & 1 & 0 \\ 0 & -\jmath & 0 & -\jmath & 0 \\ 0 & -1 & 0 & -1 & 0 \\ 0 & \jmath & 0 & \jmath & 0 \end{array} \qquad \begin{array}{ccccc} 0 & 1 & 0 & -1 & 0 \\ 0 & -\jmath & 0 & \jmath & 0 \\ 0 & -1 & 0 & 1 & 0 \\ 0 & \jmath & 0 & -\jmath & 0 \\ 0 & 1 & 0 & -1 & 0 \\ 0 & -\jmath & 0 & \jmath & 0 \\ 0 & -1 & 0 & 1 & 0 \\ 0 & \jmath & 0 & -\jmath & 0 \end{array}$$

(a) (b)

Fig. 3. IAM-C preamble for a $2 \times X$ system, with (a) and (b) correspondig to the two transmit antennas. $M = 8$. OQPSK modulation is assumed.

B. The IAM-I Method

Nevertheless, it can be verified from (5) that one can do better in maximizing the magnitude of the pseudo-pilots if *imaginary* pilot symbols $\jmath d_{p,1}$ of maximum modulus d are also allowed in the preamble. The reason is that the corresponding pseudo-pilot would then be imaginary and hence of larger magnitude than in IAM-R, namely $|d_{p,1} + u_{p,1}|$, provided that the signs of the pilot symbol and its neighbors are properly chosen so that $d_{p,1}u_{p,1} > 0$. Such an IAM scheme was first proposed in [16], and was called IAM-I to signify the presence of imaginary pilots. The middle preamble vector consists of triplets, with each of them following the above principle, and the pilots in each triplet are otherwise selected in random and independently of the other triplets. Hence, imaginary pseudo-pilots result in only one third of the subcarriers, whereas the rest of them deliver complex pseudo-pilots of smaller magnitude, $d|(1 + \beta) + \jmath\beta|$. Fig. 2(b) shows an example for $M = 8$ and OQPSK modulation.[3]

C. The IAM-C Method

With the preamble proposed in [16], imaginary pseudo-pilots will result in only one third of the subcarriers used, whereas the rest of the subcarriers will deliver complex pseudo-pilots. With a slight modification, one can improve upon this and obtain pseudo-pilots that are either purely real or imaginary at *all* the subcarriers. The idea is to simply set the middle OFDM/OQAM symbol equal to that in IAM-R but with the pilots at the odd subcarriers multiplied by $\jmath$, as shown in [8] and independently in [7]. For the $M = 8$ OQPSK example, this will result in the preamble shown in Fig. 2(c).

IV. The MIMO Case

As in MIMO-OFDM, one can consider three different patterns for preamble training (see, e.g., [3, Section 5.7]): independent (one antenna at a time), scattered (transmitting at different frequencies), and orthogonal (transmitting orthogonal signals at the same times and frequencies). IAM preambles of the latter category can be easily constructed from their SISO counterparts if a pattern analogous to that used for MIMO-OFDM in [19] is followed.

[3]Note that this preamble, as well as the one of the following subsection, is, strictly speaking, not OQAM. Nevertheless, it can still be fed to the synthesis filter bank and perfectly reconstructed at the analysis bank.

It is clear from (9) that one will need at least N_t (nonzero) OFDM/OQAM symbols to estimate the CFR matrix. Assume the channel is time invariant during a period of $2N_\mathrm{t} + 1$ OFDM/OQAM symbols. Take the example of $N_\mathrm{t} = 2$ for the sake of simplicity. One antenna can use the same preamble used in the SISO case, but with a repetition, as shown in the example of Fig. 3(a), for IAM-C (similarly for the other IAM variants). The other antenna uses the same preamble, but with changed signs at the second nonzero OFDM/OQAM symbol (cf. Fig. 3(b)). Then writing (9) at times $q = 1, 3$ results in

$$\begin{bmatrix} \boldsymbol{y}_{p,1} & \boldsymbol{y}_{p,3} \end{bmatrix} = \boldsymbol{H}_{p,1} \begin{bmatrix} c^1_{p,1} & c^1_{p,3} \\ c^2_{p,1} & c^2_{p,3} \end{bmatrix} + \begin{bmatrix} \boldsymbol{\eta}_{p,1} & \boldsymbol{\eta}_{p,3} \end{bmatrix}$$

Taking the structure of this preamble into account and recalling the assumption about the interference being mostly contributed from the first-order FT neighbors, one can easily see that $c^1_{p,1} = c^1_{p,3} = c^2_{p,1} = -c^2_{p,3} \equiv c_p$ and hence

$$\begin{aligned} \begin{bmatrix} \boldsymbol{y}_{p,1} & \boldsymbol{y}_{p,3} \end{bmatrix} &= \boldsymbol{H}_{p,1} \begin{bmatrix} c_p & c_p \\ c_p & -c_p \end{bmatrix} + \begin{bmatrix} \boldsymbol{\eta}_{p,1} & \boldsymbol{\eta}_{p,3} \end{bmatrix} \\ &= \boldsymbol{H}_{p,1} c_p \boldsymbol{A}_2 + \begin{bmatrix} \boldsymbol{\eta}_{p,1} & \boldsymbol{\eta}_{p,3} \end{bmatrix}, \end{aligned} \tag{11}$$

where $\boldsymbol{A}_2$ is the *orthogonal* matrix

$$\boldsymbol{A}_2 = \begin{bmatrix} 1 & 1 \\ 1 & -1 \end{bmatrix}$$

and the pseudo-pilot c_p can be again pre-calculated as in the SISO case. An estimate of the CFR matrix at the subcarrier p can then be computed as

$$\begin{aligned} \hat{\boldsymbol{H}}_{p,1} &= \begin{bmatrix} \boldsymbol{y}_{p,1} & \boldsymbol{y}_{p,3} \end{bmatrix} \frac{1}{c_p} \boldsymbol{A}_2^{-1} \\ &= \boldsymbol{H}_{p,1} + \frac{1}{2c_p} \begin{bmatrix} \boldsymbol{\eta}_{p,1} & \boldsymbol{\eta}_{p,3} \end{bmatrix} \boldsymbol{A}_2 \end{aligned} \tag{12}$$

Remarks.

1) It should be noted that, in IAM-R and IAM-C, c_p's have the same magnitude at all frequencies p. Clearly, this is not true for IAM-I.
2) Note that, in view of the orthogonality of the matrix $\boldsymbol{A}_2$, noise enhancement is again controlled by the magnitude of the pseudo pilot c_p. Indeed, one can readily see that the covariance matrix of the noise term in (12) equals $\frac{\sigma^2}{|c_p|^2} \boldsymbol{I}_{N_\mathrm{r}}$, which corresponds to a MSE given by

$$E\left(\|\boldsymbol{H}_{p,1} - \hat{\boldsymbol{H}}_{p,1}\|^2 \right) = N_\mathrm{r}\sigma^2/|c_p|^2 \tag{13}$$

3) The preamble above is easily generalized to systems with more than two transmit antennas, with N_t being a power of 2. Simply select the corresponding matrix $\boldsymbol{A}_{N_\mathrm{t}}$ to be a Hadamard matrix of order N_t and build the preamble accordingly. The MSE will be still given by (13).
4) For an $N_\mathrm{t} \times N_\mathrm{r}$ system, the preamble requires $2N_\mathrm{t} + 1$ OFDM/OQAM symbols. This is equivalent to $N_\mathrm{t} + 1/2$ complex OFDM/QAM symbols, that is, half a complex symbol longer than the preamble one would use in MIMO-OFDM. Nevertheless, even this extra OQAM symbol can be avoided in practice, by eliminating the leading null symbol in the preamble above. This is often possible when interference from preceding data can be practically ignored, as for example in WiMAX [3], where the gap between two successive frames can play the role of the missing guard symbol.
5) Eq. (11) relies on the assumption that the prototype filter is sufficiently well localized in time so that interference from times other than the previous and next is negligible. In fact, this is often not the case in practice and there is nonnegligible interference to the (p, q) FT point from $(p \pm 1, q \pm 2)$ as well. Hence the "pseudo pilot" matrix in (11) is equal to $\begin{bmatrix} c_p^1 & c_p^1 \\ c_p^2 & -c_p^2 \end{bmatrix}$ instead, with c_p^i corresponding to the ith transmit antenna and $|c_p^1| \neq |c_p^2|$. The latter implies that the two columns of the CFR matrix (i.e., the channels from the two transmit antennas) are not estimated with the same accuracy. The associated MSE for the subcarrier p is then equal to $\frac{N_\mathrm{r}\sigma^2}{2}\left(\frac{1}{|c_p^1|^2} + \frac{1}{|c_p^2|^2}\right)$. Things are analogous, yet somewhat more complicated, for $N_\mathrm{t} > 2$. In general, the pseudo pilot matrix is no longer unitary. It only has (nearly) orthogonal rows. This fact was taken into account in the simulations, that is, the correct (not the ideal) pseudo pilot matrix was used in all cases.

V. Simulation Results

In this section, simulation results are reported that demonstrate the estimation performances of the MIMO IAM schemes discussed above. For the sake of completeness, CP-OFDM is also included, with the minimum possible CP length (=channel order). A realistic scenario where the preambles are followed by pseudo-random data was considered. Thus, the late part of the preamble signal contains a portion of the front tail of the data burst as well, and *this was taken into account when estimating the transmit power required.*

The experiments utilized prototype filters designed as in [5]. QPSK modulation was adopted. The CP-OFDM preamble was similarly chosen, namely $\boldsymbol{A}_{N_\mathrm{t}} \otimes \boldsymbol{x}$ with $\boldsymbol{x}$ being a pseudo-random M-vector of complex QPSK pilots. The normalized MSE, $E\left(\frac{\|\boldsymbol{H} - \hat{\boldsymbol{H}}\|^2}{\|\boldsymbol{H}\|^2}\right)$ is plotted with respect to the signal to noise ratio (SNR). The latter is defined as the ratio of the average power of the channel inputs (i.e., SFB outputs) to the power of the noise. Note that in order to be fair with respect to the power transmission requirements, all the preambles are appropriately scaled so as to result in the *same* average power *at the SFB outputs*. It must be emphasized that although the IAM preambles under study are of the same power at the SFB input, their powers differ considerably after the modulation. An example is shown in Fig. 4. The figure also shows that, as pointed out in [14], this kind of IAM preambles result in high PAPR signals at the SFB output due to their deterministic/periodic nature. In fact, as it can be seen in the example, this effect is more evident in IAM-C than in IAM-R, while it is much less severe in IAM-I due to its pseudorandom symbols. These peaks were included in the average power estimates of the corresponding channel inputs.

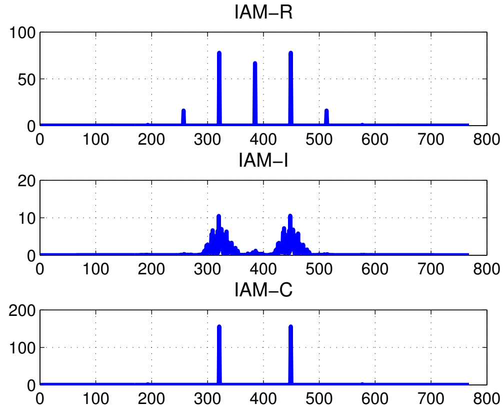

Fig. 4. Magnitude squared of the modulated IAM preambles at the first antenna of a $2 \times X$ system. $M = 128$, $K = 4$. QPSK modulation.

The channel taps were modeled in accordance with the Kronecker model, that is $\boldsymbol{h}(l) = \boldsymbol{R}_\mathrm{r}^{1/2}(l)\boldsymbol{h}_\mathrm{w}(l)\boldsymbol{R}_\mathrm{t}^{1/2}(l)$, $l = 0, 1, \ldots, L_h - 1$, where the receive and transmit correlation matrices $\boldsymbol{R}_\mathrm{t}(l), \boldsymbol{R}_\mathrm{r}(l)$ are generated according to the exponential model, and $\boldsymbol{h}_\mathrm{w}(l)$ is a matrix of i.i.d. zero mean circularly symmetric Gaussian entries with their variance following a given (Veh-A or Veh-B) power delay profile. Weak spatial correlation was assumed at both the transmit and receive sides of the channel.

Fig. 5 shows the MSE performance of the methods under study in 2×2 systems, with $M = 256$ subcarriers and an overlapping factor of $K = 4$. Channels of the Veh-A and Veh-B types are considered in Figs. 5(a) and (b), respectively. Observe that IAM-C outperforms the other schemes in the whole SNR range considered. Moreover, all the IAM methods perform better than CP-OFDM for low to moderate SNR values. At higher SNRs, CP-OFDM takes over while the MSE curves of the IAM schemes exhibit an error floor. This is a well known phenomenon in FBMC/OQAM and is due to the fact that the approximation (4) is not exact for channels of significant time dispersion. Hence there is residual intrinsic interference, which is hidden by the noise at low SNRs and shows up in the weak noise regime. It should also be noticed that IAM methods are less well performing with Veh-B channels and the crossing point with the CP-OFDM curve appears earlier in that case (see Fig. 5(b)). This behavior is again explained by the fact that, in the highly frequency

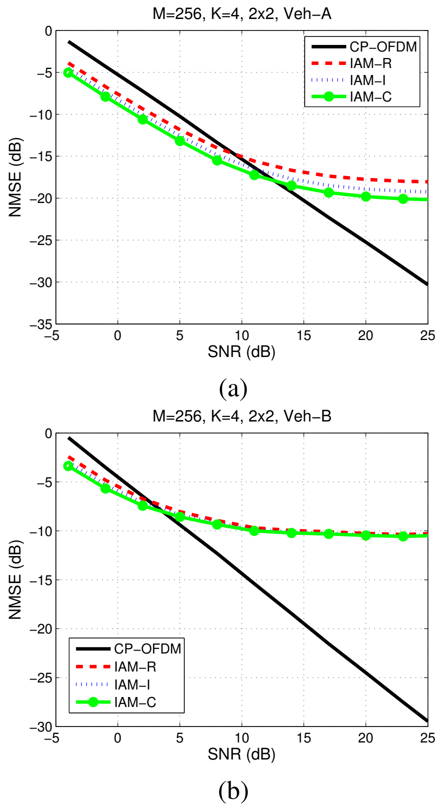

Fig. 5. MSE performance for a 2×2 OFDM/OQAM system with $M = 256$, $K = 4$, and (a) Veh-A and (b) Veh-B channel models.

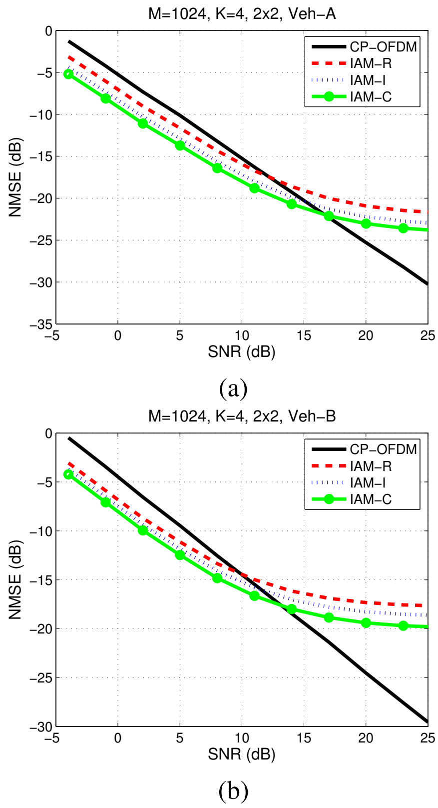

Fig. 6. As in Fig. 5, with $M = 1024$.

selective Veh-B case, the assumption of a locally flat CFR is much less valid. Increasing the number of subcarriers however, subchannels become closer to being frequency flat and the crossing point with CP-OFDM moves to the right as one can see in Fig. 6, where prototype filters of the same type but with $M = 1024$ were employed.

References

[1] P. Achaichia, M. Le Bot, and P. Siohan, "Windowed OFDM versus OFDM/OQAM: A transmission capacity comparison in the HomePlug AV context," *Proc. ISPLC'11*, Udine, Italy, 3–6 April 2011.

[2] P. Amini, R. Kempter, and B. Farhang-Boroujeny, "A comparison of alternative filterbank multicarrier methods for cognitive radio systems," *Proc. SDR'06,* Orlando, FL, 13–17 Nov. 2006.

[3] J. G. Andrews, A. Ghosh, and R. Muhamed, *Fundamentals of WiMAX: Understanding Broadband Wireless Networking*, Prentice-Hall, 2007.

[4] F. Bader and M. Shaat, "Pilot pattern adaptation and channel estimation in MIMO WiMAX-like FBMC system," *Proc. ICWMC'10*, Valencia, Spain, 20–25 Sept. 2010.

[5] M. G. Bellanger, "Specification and design of a prototype filter for filter bank based multicarrier transmission," *Proc. ICASSP'01*, Salt Lake City, UT, 7–11 May 2001.

[6] N. Benvenuto *et al.*, "Analysis of channel noise in orthogonally multiplexed OQAM signals," *Proc. GLOBECOM'93*, Houston, TX, 29 Nov–2 Dec. 1993.

[7] Deliverable D4.1: "MIMO channel estimation and tracking," *PHYDYAS document* (online) http://www.ict-phydyas.org/delivrables/PHYDYAS-D4.1.pdf/view.

[8] J. Du and S. Signell, "Novel preamble-based channel estimation for OFDM/OQAM systems," *Proc. ICC'09*, Dresden, Germany, 14–18 June 2008.

[9] J. Du, *Pulse shape adaptation and channel estimation in generalized frequency division multiplexing systems*, Licentiate thesis, KTH, Dec. 2008.

[10] B. Farhang-Boroujeny, "OFDM versus filter bank multicarrier," *IEEE Signal Processing Magazine*, pp. 92–112, March 2011.

[11] J.-P. Javaudin and Y. Jiang, "Channel estimation in MIMO OFDM/OQAM," *Proc. SPAWC'08*, Recife, Brazil, 6–9 July 2008.

[12] —–, "Channel estimation for iterative MIMO OFDM/OQAM transceivers," *Proc. EW'08*, Prague, Czech Republic, 22–25 June 2008.

[13] J.-P. Javaudin, D. Lacroix, and A. Rouxel, "Pilot-aided channel estimation for OFDM/OQAM," *Proc. VTC'03 (Spring)*, Jeju Island, Korea, 26–29 April 2003.

[14] C. Lélé, *OFDM/OQAM Modulation: Channel Estimation Methods, and Applications to Multicarrier CDMA and Multi-antenna Transmission*, Ph.D. thesis, CNAM, 2008.

[15] C. Lélé *et al.*, "Channel estimation methods for preamble-based OFDM/OQAM modulations," *European Trans. Telecommunications*, pp. 741–750, 2008.

[16] C. Lélé, P. Siohan, and R. Legouable, "2 dB better than CP-OFDM with OFDM/OQAM for preamble-based channel estimation," *Proc. ICC'08*, Beijing, China, 19–23 May 2008.

[17] F. Schaich, "Filter bank based multicarrier transmission (FBMC) – evolving OFDM," *Proc. EW'10*, Lucca, Italy, 12–15 April 2010.

[18] P. Siohan, C. Siclet, and N. Lacaille, "Analysis and design of OFDM/OQAM systems based on filterbank theory," *IEEE Trans. Signal Processing*, vol. 50, no. 5, pp. 1170–1183, May 2002.

[19] G. L. Stüber *et al.*, "Broadband MIMO-OFDM wireless communications," *Proc. IEEE*, vol. 92, no. 2, pp. 271–294, Feb. 2004.

[20] R. van Nee and R. Prasad, *OFDM for Wireless Multimedia Communications,* Artech House Publ., 2000.